Polymerization-induced phase separation

J. C. Lee
Department of Physics and Astronomy, University of Southern Mississippi, Hattiesburg, Mississippi 39406-5046
(Received 27 January 1999)

A molecular dynamics simulation is performed to study the kinetics of microphase separation in a polymer-dispersed-liquid-crystal forming process. An equimolar mixture of monomers and liquid crystal molecules are thermalized in a well mixed state. The monomers are then polymerized at the same temperature. The end product is a spanning gel with liquid crystal molecules aggregating in droplets here and there. The peak position of the equal-time structure function suggests that the growth of the droplets may be described with $t^{-0.23}$. The small growth exponent is just one of several features which may be attributed to the growing elastic gel. We argue that the aggregation is driven by entropy. [S1063-651X(99)02408-3]

PACS number(s): 61.41.+e, 61.30.−v, 64.75.+g

I. INTRODUCTION

Polymer dispersed liquid crystal (PDLC) is a composite material of considerable technological importance [1]. It consists of liquid crystal droplets dispersed in a polymer matrix. One way of fabricating PDLC is to prepare a homogeneous mixture of polymer and liquid crystal (LC), and then change the temperature so that the two components of the mixture are no longer miscible. This method is called temperature-induced phase separation (TIPS) [2]. In another method called polymerization-induced phase separation (PIPS) [3–9], the initial mixture consists of monomers and LC, and the phase separation is induced by polymerizing the monomers. The kinetics of PIPS is the focus of the present investigation.

The kinetics of PIPS has been studied experimentally [3,9] and theoretically [3,4]. According to the results by Kim *et al.* [3], light scattering exhibits all the characteristics of spinodal decomposition or TIPS [2]. The peak position of the scattering intensity moves towards the direction of the smaller angle following the power-law pattern of $t^{-\alpha}$ with $\alpha=1/3$ at early times and $\alpha=1$ at late times, and accordingly the results for $S(q,t)$ follow dynamic scaling. Thus the decomposition is due to diffusion at early times and hydrodynamic effects at late times. Kim *et al.* also find a cascade phenomenon in the microphase separation process, where small new droplets emerge after those of the first generation have grown to a rather large size. Except for this last feature, the kinetics of this system is remarkably similar to that of the spinodal decomposition in binary liquid mixtures [10].

This is in accordance with the picture that Lin and Taylor [4] propose for the kinetics of PIPS. Lin and Taylor argue in the following way. In TIPS, the system temperature is reduced from the one-phase region to the two-phase region. In PIPS, on the other hand, the temperature remains unchanged but the binodal and spinodal lines are progressively pushed up as the polymerization proceeds, and the phase separation begins when the lines surpass the system temperature. While this provides a convenient and insightful picture, it does not mean that the kinetics is always the same as in TIPS. The shape of the lines can change as the lines are pushed up, and as a result some exotic phenomenon can take place such as the nucleation-initiated spinodal decomposition [11] which is inconceivable in any TIPS.

Golemme *et al.* [9] have extended the experiment with many more samples. Their results show that the growth kinetics is quite different depending on the concentration of the liquid crystal ϕ_{LC}. When ϕ_{LC} is high, the late time growth exponent is close to what Kim *et al.* observed, but when ϕ_{LC} is lower than 60% in weight, the exponent plunges well below 0.5. Moreover, the time evolution of the structure factor does not grow exponentially, which contradicts the prediction of the linearized Cahn-Hilliard theory [12]. Thus when the LC concentration is very low, the kinetics is not exactly as envisioned by Lin and Taylor.

There are two important time scales in PIPS: t_{pl} represents the polymerization process while t_{ps} represents the phase separation process. The Lin-Taylor picture is based on the assumption that $t_{\mathrm{pl}} \gg t_{\mathrm{ps}}$. For the samples used by Kim *et al.* and Golemme *et al.*, this condition is approximately met. What if $t_{\mathrm{pl}} \ll t_{\mathrm{ps}}$? This is true of the two time scales in the case of the samples used by Serbutoviez *et al.* [7]. Serbutoviez *et al.* use the photopolymerization method while Kim *et al.* and Golemme *et al.* use the thermal reaction method; the former is a much faster polymerization method than the latter. Thus the gelation process precedes the phase separation process. Another important difference is that Serbutoviez *et al.* only use tetrafunctional monomers for the polymer component, while Kim *et al.* and Golemme *et al.* use both trifunctional and bifunctional monomers; the gel is therefore more rigid in the former than in the latter.

Serbutoviez *et al.* did not measure the time evolution of the structure factor and it remains unknown how the kinetics is affected when network elasticity begins to play a dominant role. It is useful to know that Serbutoviez *et al.* rarely find droplets coalescing if the system is left at the same curing temperature. This suggests a very slow kinetics. Computer simulation has been performed by Chen and Chen [6], and by Teixeria and Mulder [8] for the kinetics of PIPS, but their models do not allow any elastic effect of the gel network. We shall perform a molecular dynamics simulation with a more realistic molecular model which should allow both hydrodynamic and elastic effects, if any.

II. MODEL

Assuming that the rodlike structure of LC molecules has no important effect on the microphase separation pattern, we

represent both monomers and LC molecules as simple Lennard-Jones molecules. The LC-LC and monomer-monomer pair interactions are both given by $4\epsilon\{(\sigma/r)^{12}-(\sigma/r)^{6}\}$, while the LC-monomer pair interaction is given by $4\epsilon\{(\sigma/r)^{12}-0.6(\sigma/r)^{6}\}$. Since the van de Waals tail is weaker in the interspecies interaction than in the intraspecies interaction, the initial mixture has a normal phase diagram with an upper critical temperature. To simplify the computation further, we also assume that both species have the same mass m. These assumptions will alter time scales, but we assume that the micro phase separation pattern will remain unaltered.

For the polymerization process [13], the majority of the monomers are trifunctional (meaning that they can support a maximum of three bonds) and a very small portion is bifunctional. Initially a certain number of monomers are chosen randomly as active monomers. If an active monomer comes within the prescribed distance $R_{\min}$ of another monomer which has at least one functionality left, a bond is formed between the two. If the latter was not active before the encounter, it now becomes active while the initial active monomer becomes inactive. If both were active, on the other hand, both become inactive after the chemical reaction. The polymerization process stops soon because there are not enough active monomers left and those still remaining active are at wrong places. This makes the local gel structure quite different depending on whether the local bonds are formed early or late. To prevent this highly heterogenous structure from developing, we periodically activate more monomers. If the current number of active monomers is less than the initial value by n, we randomly select n inactive monomers. Among them, only those which have at least one functionality left become activated. In the language of photopolymerization, we send the activating light beam periodically.

The bond potential can be written in several different ways, one of which is the FENE potential [14]

$$\phi(r)=\begin{cases}-0.5KR_0^2\ln[1-(r/R_0)^2], & r\leqslant R_0\\ 0, & r\geqslant R_0.\end{cases} \tag{1}$$

It is a harmonic potential whose effective spring constant increases with r via $k/[1-(r/R_0)^2]$. The potential well is infinitely steep at $r=R_0$, and therefore once a bond is formed, it does not break. In the present system, the gelation process takes place in the presence of LC molecules. Since two monomers cannot form a bond if an LC molecule is between them, LC molecules play a role in determining where to form bonds. They also move around, which should have the effect of stabilizing certain parts of the gel while destabilizing other parts. The stress on the latter part could be massive, and it appears unreasonable to assume that all bonds will be able to support the stress no matter how massive the stress may be. Thus we modify the bond potential so as to allow the possibility of bond breaking:

$$\phi(r)=\begin{cases}-0.5KR_0^2\ln[1-(r/R_0)^2], & r\leqslant R_1\leqslant R_0\\ 0, & r\geqslant R_1.\end{cases} \tag{2}$$

The bonds break if they are stretched beyond R_1.

PDLC is a thin film, but its thickness is more than a few intermolecular distances, and therefore it is a three-dimensional system. A two-dimensional model would require much less CPU to simulate, but a two-dimensional PDLC model can be quite misleading. To see why, consider a long chain of monomer molecules on a plane. LC molecules cannot cross over the chain and therefore the absence of the third dimension alters the molecular motions quite significantly. We choose a slab, which is thick enough to allow a molecule to go over another for horizontal motions. The problem would remain if the chain is thick enough to take up the entire vertical extension of the slab. It is to minimize this possibility that we choose the trifunctional monomers rather than tetrafunctional monomers.

A total of 7500 molecules are placed in a self-closed slab (with periodic boundary conditions) of $L_x\times L_y\times L_z$, where $L_x=L_y\equiv L=50$, and $L_z=3$, in units of σ; the density is 0.85. Of the 7500 molecules, half are monomers and half are LC molecules. Among the monomers, 97% are trifunctional and 3% bifunctional. The initial fraction of the active monomers is 34.3%. For the spring, $R_0=1.5\sigma$, $R_1=1.47\sigma$, $K=30.0\epsilon/\sigma^2$, and $R_{\min}=0.9\sigma$. The reduced temperature having been set at $k_BT/\epsilon=7.47$, the initial mixture is quite safely in the one-phase region. At this temperature, the chance of the thermal energy's breaking a bond is approximately $e^{-12.57}$. Only when a few ill-conceived bonds have to support a massive stress in the gel, can the bonds break.

The molecular positions and velocities are updated for each time increment of $\delta t=0.004$ in the units of $\tau=(m\sigma^2/48\epsilon)^{1/2}$. When t advances by δt on a Pentium II machine, the wall clock advances by 0.0345 sec.

The initial mixture is thoroughly thermalized before the polymerization process begins. As the polymerization proceeds, we measure at various times the equal-time structure factor

$$S(q,t)=\langle\rho(q,t)\rho(-q,t)\rangle/2N, \tag{3}$$

where $N=7500$ and t is the elapsed time from the moment the polymerization began. We write the concentration fluctuation $\rho(q,t)$ in the form of

$$\rho(q,t)=\sum_{\alpha i}\exp(i\vec{q}\cdot\vec{r}_{\alpha i})-\sum_{\beta i}\exp(i\vec{q}\cdot\vec{r}_{\beta i}), \tag{4}$$

where α stands for the monomers and β the LC molecules, and the negative sign in the second term provides a dielectric contrast between the two species. The probed wave vectors are $q=2\pi k/L$ where $k=2,3,4,\ldots,18$. For the ensemble average, 29 runs are made with different initial configurations.

III. RESULTS AND DISCUSSION

Figures 1, 2, and 3 are the snapshots taken at $t=4$, $t=8$, and $t=460$, respectively. Figure 4 shows the number of bonds formed by t while Fig. 5 shows those broken by t. A spanning gel is visible in Fig. 1 and a nearly completed gel in Fig. 2. The gel structure, however, continues to change in an important way after Fig. 2. Approximately 20% of the tetrafunctional monomers in Fig. 2 still have one or two functionalities left. What happens after Fig. 2 is that these functionalities are gradually exhausted to make the gel structure even more rigid. At no time can the gel structure be regarded as cross-linked chains.

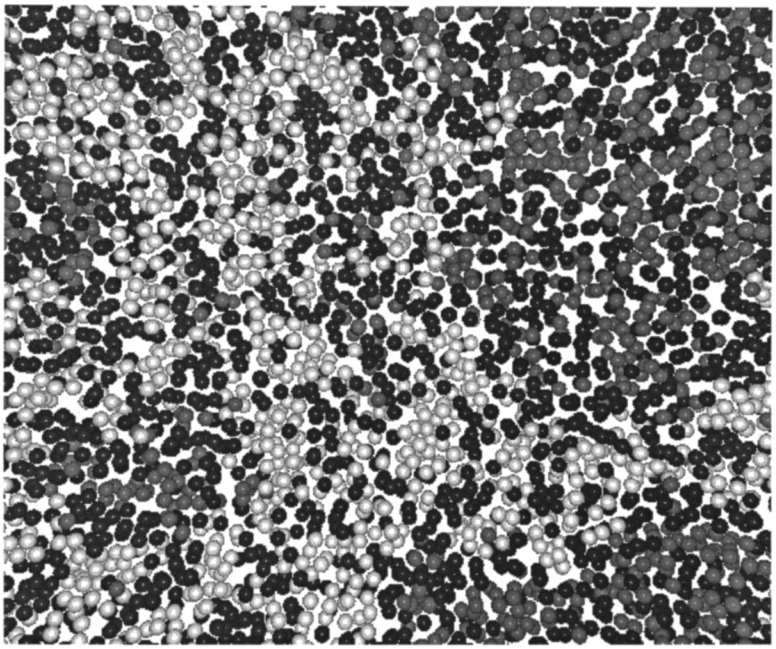

FIG. 1. The molecular morphology at $t=4$ (in units of τ): LC molecules are in the dark shade, the monomers forming the spanning gel are in light gray, and those that have not yet joined the spanning gel in a medium gray. Approximately 60% of the molecules are in the camera view.

For each realization of the sample, the results for $S(q,t)$ often exhibit a few towering local peaks. These peaks appear at different places in different realizations, which requires a large ensemble to obtain a smooth function. With an ensemble of size 29, the result is good enough to exhibit a gross pattern with one peak, but it is not good enough to allow us to read off the peak position directly. It is therefore necessary to fit the data. Figure 6 shows the fitted data points as a function of k. The time evolution appears to exhibit what is generally regarded as the hallmark of spinodal decomposition. There is a peak at a finite wave vector. The peak position moves toward the direction of the smaller wave vector and the peak intensity increases as time progresses.

In Fig. 7, we have plotted the raw data for $S(k,t)$ as a function of t. In the results for small wave vectors, it is clear that the time evolution is not exponential as predicted by the linearized Cahn-Hilliard theory for the early time decomposition. In this important detail, the time evolution of $S(k,t)$ does not follow what is expected of the spinodal decomposition. The result is more similar to what Golemme *et al.* observe when the liquid crystal concentration is very low. In the results for large wave vectors, the intensity reaches its maximum quite early and then remains with little or no change. The apparent equilibrium does not mean that the small-length-scale structures do not grow into large-length scale structures. They do, but they are continuously replenished by new batches of nucleation. The experimental results by Kim *et al.* show the same feature more convincingly. We propose to regard it as a continuous cascade phenomenon. It shows that the relaxation time of the LC molecules in the growing gel is spread over a wide range.

In Fig. 8, the peak position k_{mx} of $S(k,t)$ is plotted as a

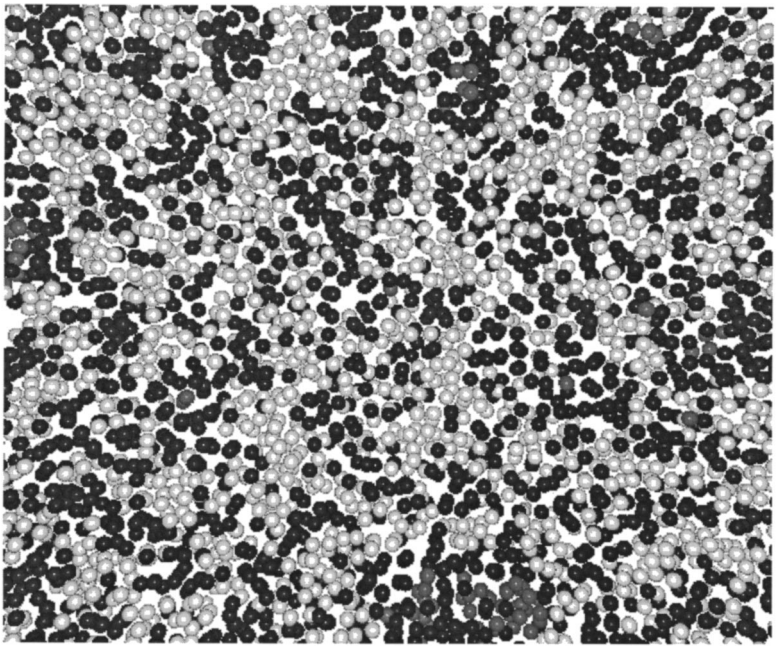

FIG. 2. The molecular morphology at $t=8$ (in units of τ): LC molecules are in the dark shade, the monomers forming the spanning gel are in light gray, and those that have not yet joined the spanning gel are in a medium gray.

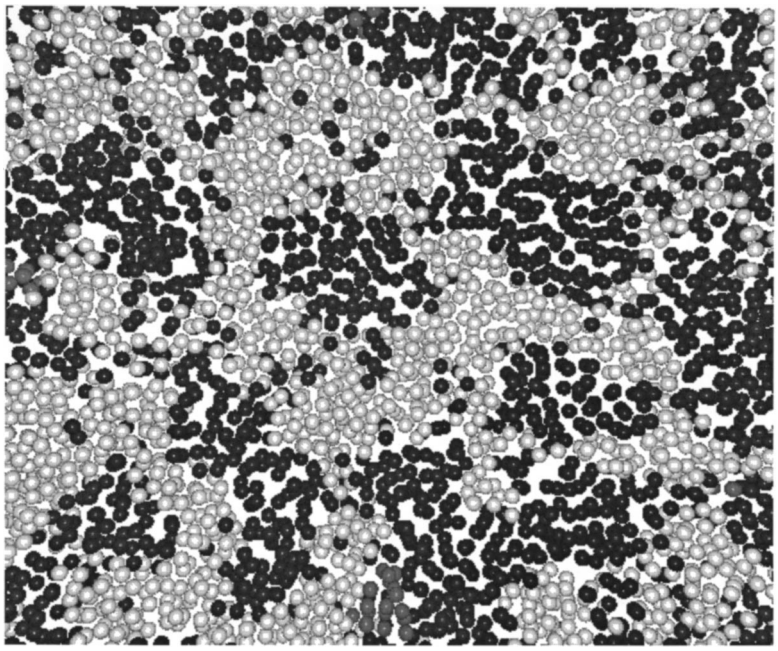

FIG. 3. The molecular morphology at $t=460$ (in units of τ): LC molecules are in the dark shade, the monomers forming the spanning gel are in light gray, and those that have not yet joined the spanning gel are in a medium gray.

function of t. The overall growth pattern may be approximated in the form of $t^{-0.23}$. The growth exponent is in the range observed by Golemme *et al.* when the LC concentration is low. The low growth exponent reflects how difficult it is for the LC molecules to aggregate in the midst of the rigid gel network.

The length scale that the peak position represents grows with time. Does this length scale dominate the kinetics? If so, one could expect the results for $S(q,t)$ to support scaling of the form

$$S(k,t)/S(k_{mx},t)=F(k/k_{mx}), \tag{5}$$

where k_{mx} is a function of t. Figure 9 shows the scaling plot. Except for very early times, the results do indeed support the scaling.

Why do the LC molecules aggregate? We have thoroughly tested and confirmed that the initial mixture remains mixed so long as the monomers are not polymerized. The aggregation is entirely due to the polymerization. It is an entropy-driven phenomenon in much the same way as in the colloidal aggregation [15]. Consider the LC molecules trapped in the growing gel at early times. When bonds are formed and trap the LC molecules, they effectively freeze the positional entropy of the LC molecules. Should the LC molecules overcome the energy barriers posed by the gel net-

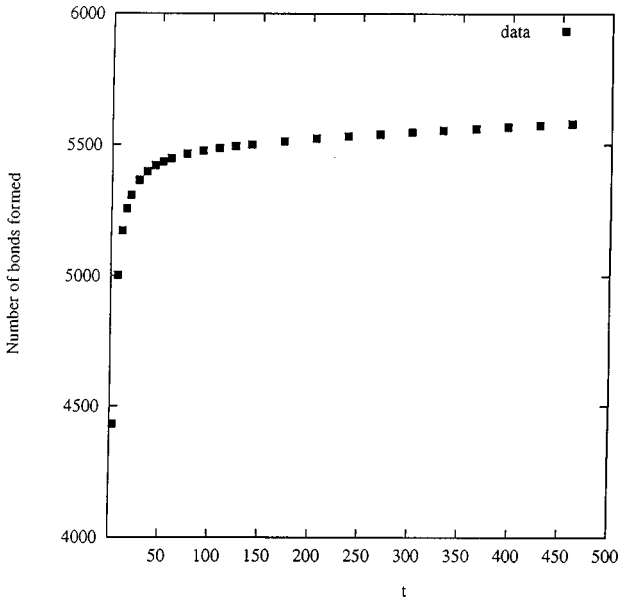

FIG. 4. The total number of bonds formed by time t (in units of τ.)

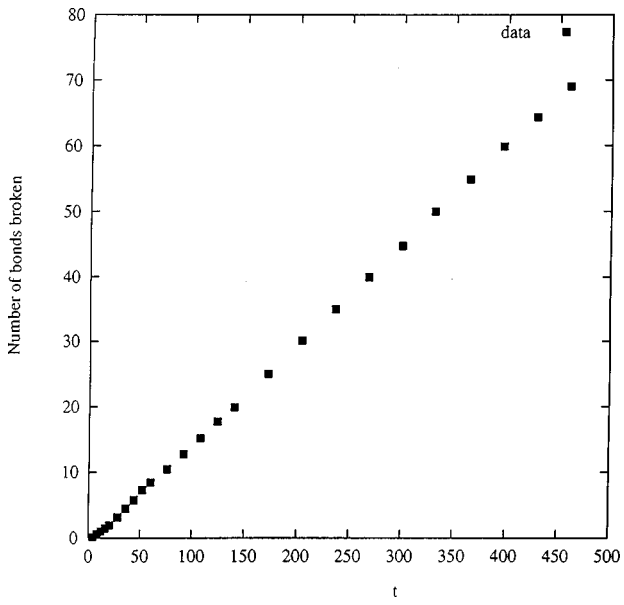

FIG. 5. The total number of bonds broken by time t (in units of τ).

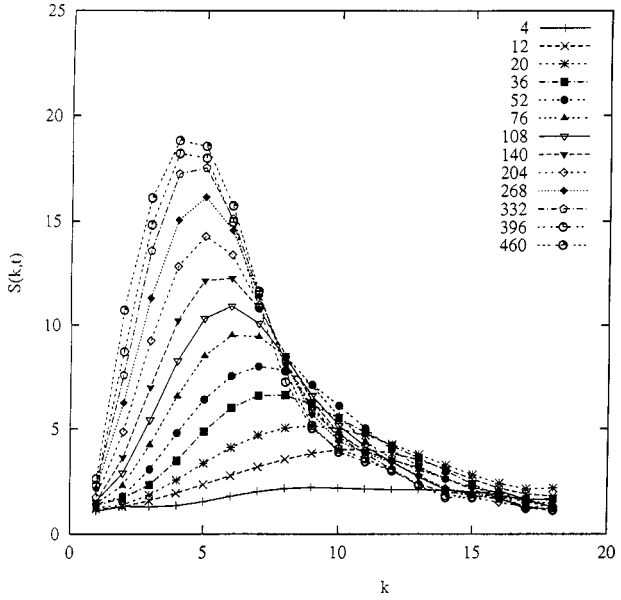

FIG. 6. $S(k,t)$ plotted vs k for the values of t (in units of τ) shown in the legend.

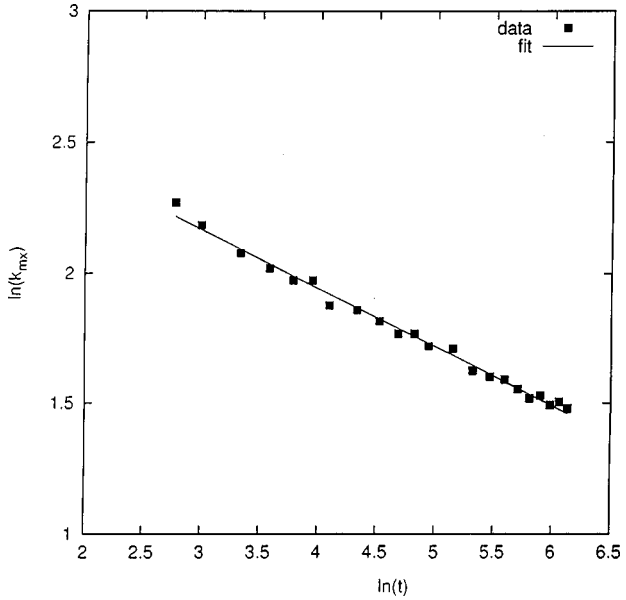

FIG. 8. ln-ln plot of k_{mx} vs t (in units of τ).

work and aggregate, the small bits of space that they previously occupied would be removed for much larger pieces of space accessible to many LC molecules. The gel and LC molecules do just that to increase their entropy when they form droplets.

It is the bonds which provide the entropy incentive. Should we remove all the bonds in the gel at any moment, the entropy would no longer be frozen and the LC molecules would not gain any more entropy by aggregating. To be precise, however, it is not just the bonds which provide the entropy incentive, but also the fact that the LC molecules interact with the polymer via the Lennard-Jones potential. This is because the LC molecules could not be trapped if they were free from the constraints that the Lennard-Jones interactions impose on them. Thus the two interactions conspire to provide the entropy incentive.

The gel poses to the LC molecules rugged energy barriers with hills and valleys throughout the volume. The height of these energy barriers should be distributed over a range, and so should the relaxation time of the LC molecules necessary to overcome the barriers. Some LC molecules should therefore take less time to overcome the barrier while others take more time. This is the reason for the continuous cascade phenomenon.

The energy landscape changes constantly. More hills are added when new bonds are formed. Some hills are removed when bonds are broken. Some hills are conveniently shifted or deformed when the gel network changes its shape. In these ways, the paths of the LC molecules to droplets are made rugged and tortuous, but we emphasize again that it is actually these hills that cause the droplets. Molecules pay the required energy cost for the entropy incentive, which is the

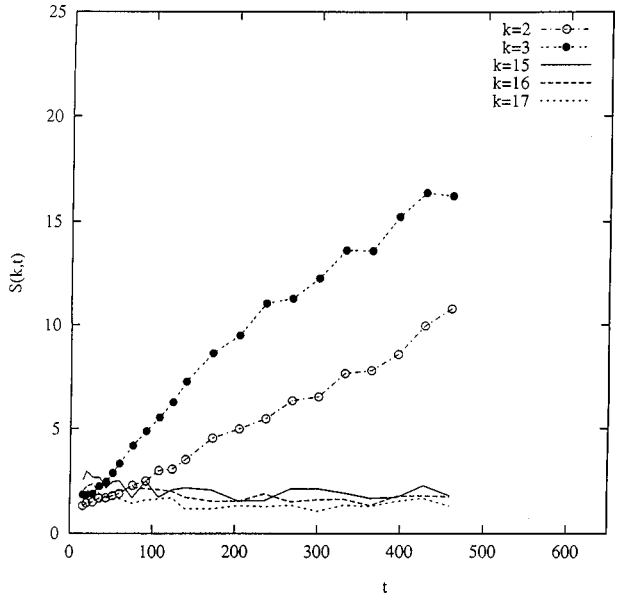

FIG. 7. $S(k,t)$ plotted vs t (in units of τ) for the values of k shown in the legend.

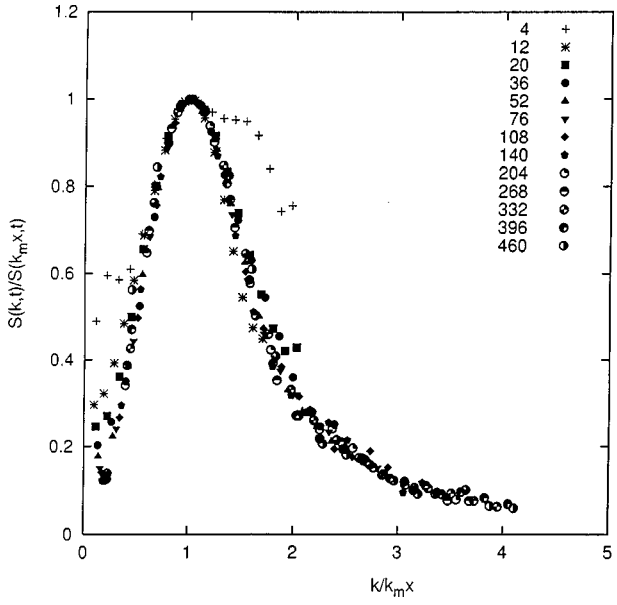

FIG. 9. The scaling plot for $S(k,t)$ for the values of t (in units of τ) shown in the legend.

reason for the unique nucleation and growth processes in this system. The surface tension, diffusion, and hydrodynamics all play little or no role. To see why, return to Fig. 1 and notice that there are several small LC clusters whose surroundings are almost completely depleted of LC molecules. Suppose that these nucleated clusters grow via the usual nucleation-and-growth mechanism. To do so, the depletion should result in a local imbalance in the chemical potential of LC molecules to force more LC molecules to diffuse into the depleted region from further distant surroundings. In the present system, the depleted region is a part of the growing gel, and the bonds are such a dominant factor that the depletion does not decrease the local chemical potential for the LC molecules. If an LC molecule enters there, the transport is an activated process; if diffusion and hydrodynamics play a role at all, it should be negligible.

To conclude, we have observed several characteristic features when LC molecules aggregate in a rather rigid gel network. It is hoped that these characteristics will prove helpful in the future in formulating a successful model for this highly nonequilibrium dynamic process.

ACKNOWLEDGMENTS

The author's venture into this topic was possible thanks to many experienced workers who kindly answered his numerous questions. He thanks J. Whitehead, C. Hoyle, G. Crawford, D. McCain, P. Palffy-Muhoray, T. Kyu, and A. Liu. This research was supported by a grant from the U.S. Air Force Office of Scientific Research.

[1] J. W. Doane, A. Golemme, J. L. West, J. B. Whitehead, and B. G. Wu, Mol. Cryst. Liq. Cryst. **165**, 511 (1988); J. L. West, *ibid.* **157**, 427 (1988); P. S. Drzaic, *Liquid Crystal Dispersions* (World Scientific, Singapore, 1995); *Liquid Crystals in Complex Geometries*, edited by G. P. Crawford and S. Zumer (Taylor and Francis, New York, 1996).

[2] T. Nagaya, H. Orihara, and Y. Ishibashi, J. Phys. Soc. Jpn. **58**, 3600 (1989); A. J. Liu, Liq. Cryst. Today **7**, 1 (1997); T. Kyu and P. Mukherjee, Liq. Cryst. **3**, 631 (1998).

[3] J. Y. Kim, C. H. Cho, P. Palffy-Muhoray, M. Mustafa, and T. Kyu, Phys. Rev. Lett. **71**, 2232 (1993).

[4] J.-C. Lin and P. L. Taylor, Mol. Cryst. Liq. Cryst. **237**, 25 (1993).

[5] G. W. Smith, Mol. Cryst. Liq. Cryst. **225**, 113 (1993); Phys. Rev. Lett. **70**, 198 (1993).

[6] W.-J. Chen and S.-H. Chen, Phys. Rev. E **52**, 5696 (1995); S.-H. Chen and W.-J. Chen, Physica A **221**, 216 (1995).

[7] C. Serbutoviez, J. G. Kloosterboer, H. M. Boots, and F. J. Touwslager, Macromolecules **29**, 7690 (1996); H. M. J. Boots, J. K. Kloosterboer, C. Serbutoviez, and F. J. Touwslager, *ibid.* **29**, 7683 (1996).

[8] P. I. C. Teixeira and B. M. Mulder, Phys. Rev. E **53**, 1805 (1996).

[9] G. Golemme, A. Urso, B. C. De Simone, A. Mashin, and G. Chidichimo, Liq. Cryst. **24**, 563 (1998).

[10] E. Siggia, Phys. Rev. A **20**, 595 (1979).

[11] T. Kyu and J.-H. Lee, Phys. Rev. Lett. **76**, 3746 (1996).

[12] J. W. Cahn and J. E. Hilliard, J. Chem. Phys. **28**, 258 (1958); **31**, 688 (1959); J. W. Cahn, *ibid.* **42**, 93 (1965).

[13] H. J. Hermann, D. Stauffer, and D. P. Landau, J. Phys. A **16**, 1221 (1983).

[14] See, for example, K. Binder, in *Monte Carlo and Molecular Dynamics Simulations in Polymer Science*, edited by K. Binder (Oxford University Press, Oxford, 1995); G. Grest and K. Kremer, Phys. Rev. A **33**, 3628 (1986).

[15] See, for example, R. Verma, J. C. Crocker, T. C. Lubensky, and A. G. Yodh, Phys. Rev. Lett. **81**, 4004 (1998).